Journal of Power Sources 194 (2009) 313–327

Contents lists available at ScienceDirect

Journal of Power Sources

journal homepage: www.elsevier.com/locate/jpowsour

# Effects of temperature uncertainty on the performance of a degrading PEM fuel cell model

Latevi Placca[a,b,c,*], Raed Kouta[a,b], Jean-François Blachot[a,c], Willy Charon[a,b]

[a] FC-Lab., Fuel Cell System Laboratory, Rue Thierry Mieg, 90000 Belfort, France
[b] M3M Research Laboratory, University of Technology of Belfort-Montbéliard, 90010 Belfort, France
[c] CEA Grenoble, DRT/LITEN/Département des Technologies Hydrogène (DTH)/Laboratoire Pile A Combustible (LPAC), 17, Rue des Martyrs, 38000 Grenoble, France

ARTICLE INFO

*Article history:*
Received 21 February 2009
Received in revised form 21 April 2009
Accepted 11 May 2009
Available online 20 May 2009

*Keywords:*
Proton exchange membrane (PEM) fuel cell
Stochastic analysis
Statistical analysis
Design under uncertainty

ABSTRACT

The performance of a fuel cell is subject to uncertainties on its operational and material parameters. Among operational parameters, temperature is one of the most influential factors. This work focuses on this parameter. A statistical analysis is developed on the output voltage of proton exchange membrane fuel cell models. The first model does not include any degradation, whereas the second one introduces a degradation rate on the cell active area. To complete the simulation work, a full factorial design is carried out and a statistical sensitivity analysis (ANOVA) is used to compute the effects and contributions of important parameters of the model on the output voltage.



## 1. Introduction

Proton exchange membrane fuel cells are considered to be reliable for transportation applications due to their low operating temperature and pressure resulting in a possible quick start-up [1,2]. The cell performance can be determined by its output voltage [3,4]. It is mainly controlled by the issues of water and thermal management [5,6]. Thus, studies on PEM modelling for improved water and thermal management were done by Bernadi and Verbrugge [7,8], Springer et al. [9,10], Baschuk and Li [11] and also Rowe and Li [12].

Then, works on parametric analysis for model based design were done by Mishra et al. [13], Mawardi et al. [14] and Min et al. [15]. Those authors considered the different parameters deterministic. Subramanyan et al. [16] were aware of the fact that operating parameters such as temperature are subject to uncertainties. Recently, design of experiment method was used for parametric analysis by Yu et al. [17] and Wu et al. [18].

A mathematical framework that incorporates all the main parameters of a cell and with most terms and coefficients derived from theory and also with empirical parameters for the changing performance is necessary for physics-based simulation and robust design. To achieve this objective, a model developed by Fowler et al. [19] will be used. For the stochastic analysis, the uncertainty on a parameter is at first quantified and then propagated through a deterministic model to build the output distribution. This latter is finally analysed for robust design objectives.

In this present work, the operating parameters with uncertainty are represented as Gaussian and uniform probability distributions. Gaussian distributions are quantified in terms of the mean and variance values and uniform distributions are quantified in terms of lower and upper bounds. A Gaussian distribution is a quasi-realistic approach whereas a uniform distribution is a severe approach. More information about these two distributions can be found in ref. [31].

Parameters are randomly generated with their respective distributions and a semi-empirical model is used for the cell operation. The results of the simulations are used to construct the probability distribution of the output voltage delivered by the cell. Parametric analysis is performed on the output voltage distribution for several values of the input parameters.

The present work is organised as follows: an introduction to uncertainty in systems engineering is described in Section 2 then the semi-empirical PEM fuel cell used for the analysis without considering degradation is described in Section 3 with its stochastical analysis and results. It is followed by the description of a new model based on the first one completed with a degradation of the cell active area in Section 4 with its stochastical analysis and results. Finally, a full factorial design of experiment is made and an analysis of variance (ANOVA) is used to compute the effects and contributions of important parameters of the model to the output voltage in Section 5.

* Corresponding author. Tel.: +33 384583654; fax: +33 384583636.
*E-mail address:* latevi-atatoe.placca@utbm.fr (L. Placca).

0378-7753/$ – see front matter © 2009 Elsevier B.V. All rights reserved.
doi:10.1016/j.jpowsour.2009.05.013

## 2. Uncertainty in systems engineering

Uncertainty plays a major role in the analysis of many fields from engineering to economics. Its concepts and ideas have been associated with gambling and games for a long time. The ancient Greeks of the 4th century BC were the first civilization having considered uncertainty primarily in the context of epistemology. In fact, the word "epistemology" is derived from the Greek "episteme", meaning "knowledge", and logos which one meaning is "theory". Epistemology considers the possibilities and limits of human knowledge. Aristotle thought that people should make decisions on the basis of "desire and reasoning to some end" but suggested no guidance to the likelihood of a successful outcome. In spite of considering uncertainty, the Greeks turned to the oracles when they wanted to predict the future [20].

In systems engineering there are two definitions for uncertainty: a rigorous and theoretical one and a more relaxed and practical one [21–23]. The rigorous definition refers to "uncertainty" as "vagueness" or "ambiguity". "Vagueness" is considered as the difficulty of making sharp and precise distinctions in the world. "Ambiguity" refers to "situations in which the choice between two or more alternatives is left unspecified." For Klir and Folger [24], ambiguity is separated into nonspecificity of evidence, dissonance in evidence, and confusion in evidence.

The practical definition refers to "uncertainty" as a distribution of outcomes with various likelihoods of both occurrence and severity. It interferes with the definition of risk which is a measure of uncertainty of achieving an objective. Risk level is determined by the probability of occurrence and the consequences of occurrence. *INCOSE Systems Engineering Handbook* [25] classify risk into technical, cost, schedule and programmatic. The two distinct classifications are in Fig. 1.

In the present work, the practical definition of uncertainty will be used.

## 3. Nondegrading PEM fuel cell model

The model used for this study is a semi-empirical model of Fowler et al. [19] giving a unique equation that links the voltage delivered by a cell to the inputs parameters. It is useful for introducing for example, a degradation rate and studying its effects on the output voltage.

### 3.1. Model mathematical equation and its validation

Starting with the general expression for the voltage for a single cell:

$$V_{\text{cell}} = E_{\text{Nernst}} + \eta_{\text{activation}} + \eta_{\text{ohmic}} \tag{1}$$

The meanings of the different terms of Eq. (1) are presented in Table 1. All quantities in Eq. (1) are in units of volts and the overvoltage terms ($\eta_{\text{activation}}$, $\eta_{\text{ohmic}}$) are all negative (Tables 2 and 3).

For a more accurate model, the concentration overvoltage term $\eta_{\text{concentration}}$ is added to Eq. (1) [26,27] but this term is not taken into account in this model because the current density $i$ will be supposed to be inferior to 1 A cm$^{-2}$ in order to prevent concentration losses.

$$E_{\text{Nernst}} = E_T^0 + \left(\frac{RT}{2F}\right) \times [\ln(P_{H_2} \times P_{O_2}^{1/2})] \tag{2}$$

Numerically, $E_T^0 = 1.229 - 0.85 \times 10^{-3}(T - 298.15)$ and replacing constants by their values, we will have the expression:

$$E_{\text{Nernst}} = 1.229 - 0.85 \times 10^{-3}(T - 298.15) + 4.31 \times 10^{-5} \times T \times [\ln(P_{H_2} \times P_{O_2}^{1/2})] \tag{2'}$$

**Table 1**
Nomenclature [19].

| | |
|---|---|
| $A$ | cell active area (cm$^2$) |
| $C^*_{H^+}$ | proton concentration at the cathode membrane/gas interface (mol cm$^{-3}$) |
| $C^*_{H_2}$ | liquid phase concentration of hydrogen at anode/gas interface (mol cm$^{-3}$) |
| $C^*_{H_2O}$ | water concentration of the cathode membrane/gas interface (mol cm$^{-3}$) |
| $C^*_{O_2}$ | oxygen concentration of the cathode membrane/gas interface (mol cm$^{-3}$) |
| $E_{\text{Nernst}}$ | thermodynamic potential (V) |
| $E_T^0$ | standard electrode potential |
| $F$ | Faraday's constant (96487 C eq.$^{-1}$) |
| $i$ | current density (A cm$^{-2}$) |
| $I$ | current (A) |
| $k_a^o$, $k_c^o$ | rate constants for the anode and cathode reactions, respectively (cm s$^{-1}$) |
| $k_{\text{cell}}$ | empirical term accounting for the apparent rate constants for the anode and cathode reactions |
| $P_{H_2}$ | partial pressure of hydrogen at anode/gas interface (atm) |
| $P_{O_2}$ | partial pressure of oxygen at the cathode membrane/gas interface (atm) |
| $l$ | thickness of the membrane layer (cm) |
| $r_M$ | membrane specific resistivity for the flow of hydrated protons ($\Omega$ cm) |
| $T$ | cell temperature (isothermal assumption in degrees K) |
| $\Delta G_e$ | standard state free energy of the cathode reaction (J mol$^{-1}$) |
| $\Delta G_{ec}$ | standard state free energy of chemisorptions from the gas state (J mol$^{-1}$) |
| $n_c$ | number of cells |
| $R^{\text{electronic}}$ | resistance to electron transfer in the graphite collector plates and graphite electrodes |
| $R^{\text{proton}}$ | resistance to proton transfer in the solid polymer membrane |
| $R^{\text{internal}}$ | internal resistance of the membrane |
| $k2$ | empirical parameter representing the ageing of the polymeric membrane (h$^{-1}$) |
| Greek letters | |
| $\alpha_c$ | chemical activity parameter for the cathode |
| $\varepsilon$ | diffusivity correction factor |
| $\eta_{\text{activation}}$ | the activation contribution to the cell activation overvoltage (V) |
| $\eta_{\text{ohmic}}$ | ohmic contribution to cell overvoltage (V) |
| $\eta_{\text{ohmic}}^{\text{electronic}}$ | electronic ohmic contribution to cell overvoltage (V) |
| $\eta_{\text{ohmic}}^{\text{proton}}$ | protonic ohmic contribution to cell overvoltage (V) |
| $\eta_{\text{concentration}}$ | concentration overvoltage (V) |
| $\xi_1, \xi_2, \xi_3, \xi_4$ | empirical coefficients for calculation of activation overvoltage |
| $\lambda$ | semi-empirical parameter representing the equilibrium water content of the membrane, $H_2O/SO_3^-$ |

$$\eta_{\text{activation}} = \xi_1 + \xi_2 T + \xi_3 T \left[\ln(c^*_{O_2})\right] + \xi_4 T[\ln(I)] \tag{3}$$

where

$$\xi_1 = -\left(\frac{\Delta G_{ec}}{2F}\right) - \left(\frac{\Delta G_e}{\alpha_c n_c F}\right) \tag{3a}$$

**Table 2**
Values of parameters used.

| |
|---|
| $P_{H_2} = 1.5$ atm |
| $P_{O_2} = 1.5$ atm |
| $\Delta G_e = 237,190$ J/mol |
| $\Delta G_{ec} = -664, 167.8$ J/mol |
| $n_c = 1$ |
| $F = 96{,}487$ |
| $k_{\text{cell}} = 0.00295$ |
| $R = 8.3147$ |
| $\alpha_c = 0.5$ |
| $A = 50$ cm$^2$ |
| $c_{H_2} = 0.85$ mol cm$^{-3}$ |
| $c_{O_2} = 0.05$ mol cm$^{-3}$ |
| $i = I/A$ |

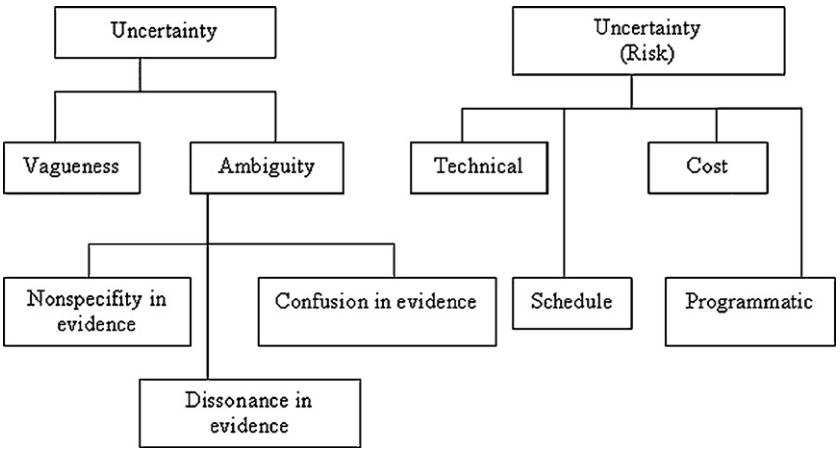


**Fig. 1.** Uncertainty classifications in systems engineering [24,25].

$$\xi_2 = \left(\frac{R}{\alpha_c n_c F}\right) \ln[n_c F A k_c^0 (c^*_{H^+})^{(1-\alpha_c)} (c^*_{H_2O})^{(\alpha_c)}] + \left(\frac{R}{2F}\right) \ln[4FAk_a^0 (c^*_{H_2})] \quad (3b)$$

$$\xi_3 = \frac{R(1-\alpha_c)}{\alpha_c n_c F} \quad (3c)$$

$$\xi_4 = -\left(\frac{R}{2F} + \frac{R}{\alpha_c n_c F}\right) \quad (3d)$$

For later use, the $\xi_2$ term in Eq. (3b) can be rewritten as the following, in order that all the rate constants for the overall reaction are grouped together in one term (which helps in the development of the degradation model):

$$\xi_2 = \left(\frac{R}{\alpha_c n_c F}\right) \ln\left[n_c F k_c^0 (c^*_{H^+})^{(1-\alpha_c)} (c^*_{H_2O})^{(\alpha_c)} (k_a^0)^{n_c \alpha_c/2}\right] + \left(\frac{R}{2F} + \frac{R}{\alpha_c n_c F}\right) \ln(A) + \frac{R}{2F} \ln\left[4F(c^*_{H_2})\right] \quad (3b')$$

$$\xi_2 = k_{cell} + 0.000197 \ln(A) + 4.3 \times 10^{-5} \ln\left(c^*_{H_2}\right) \quad (3b'')$$

The parameter $k_{cell}$ includes rate constants for the anode and cathode reactions, as well as some properties specific to the cell design such as effective catalyst surface area and the concentration of protons and water at the interface. As such, $k_{cell}$ is a measure of the apparent catalytic activity.

$$\eta_{ohmic} = \eta_{ohmic}^{electronic} + \eta_{ohmic}^{proton} \quad (4)$$

$$\eta_{ohmic} = -I(R^{electronic} + R^{proton}) \quad (4a)$$

$$\eta_{ohmic} = -IR^{internal} \quad (4b)$$

**Table 3**
RSM data.

| Factors | $t$ | $T$ | $k2$ |
|---|---|---|---|
| Minimum level | −4 | −4 | −4 |
| | −3 | | |
| | −2 | | |
| | −1 | | |
| Intermediate level(s) | 0 | 0 | 0 |
| | 1 | | |
| | 2 | | |
| | 3 | | |
| Maximum level | 4 | 4 | 4 |

According to [19],

$$R^{electronic} \ll R^{proton} \quad (4c)$$

We can write $R^{proton}$ as:

$$R^{proton} = \frac{r_M l}{A} \quad (4d)$$

$$r_M = \frac{181.6[1 + 0.03(I/A) + 0.062(T/303)^2 (I/A)^{2.5}]}{[\lambda - 0.0634 - 3(I/A)] \exp\{4.18[(T-303)/T]\}} \quad (4e)$$

Finally,

$$\eta_{ohmic} = -I \times \frac{r_M l}{A} \quad (4f)$$

The following values will be used for the unknown variables [2,19,28] for the first part of this work.

To validate the model, the voltage curve represented in Fig. 2 is compared to refs. [2,19,28], it seems to correspond to the voltage–current curve of the literature.

The graph in Fig. 2 also confirms that the voltage curve increases with the temperature, as noticed by refs. [29,30].

This model will be the basic model used for the present work.

Some parameters of the model such as temperature are subject to uncertainties [30]. In the next section, the influence of a random temperature on the output voltage will be studied by the simulation method.

### 3.2. *Effect of the temperature uncertainty on the polarisation curve*

In Fig. 3, a stochastic convergence analysis is used to determine the minimum number of numerical samples to generate randomly to reach an acceptable mean and an acceptable standard deviation of $V_{cell}$.

According to Fig. 3, a minimum of 600 random samples is sufficient to ensure the convergence to the mean and the standard deviation. 1000 numerical samples will be generated in this work.

Considering the practical definition of uncertainties in Section 2, the temperature will be assumed to follow firstly a Gaussian distribution with a mean of 353 K and a standard deviation of 3.53 K and secondly a uniform distribution with 347 and 359 K as lower and upper bounds which are acceptable referring to Santarelli et al. [28]. These values are chosen in order to have the same mean and the same standard deviation for both distributions to allow comparisons. The current density $i$ (in A cm$^{-2}$ units) takes successively the following values: 0.1, 0.2, 0.3, 0.4, 0.5, 0.6, 0.7, 0.8, 0.9 and 1.

Fig. 4 represents the voltage of the cell called '$V_{cell}$' with both cases of stochastical temperature distributions. The values of

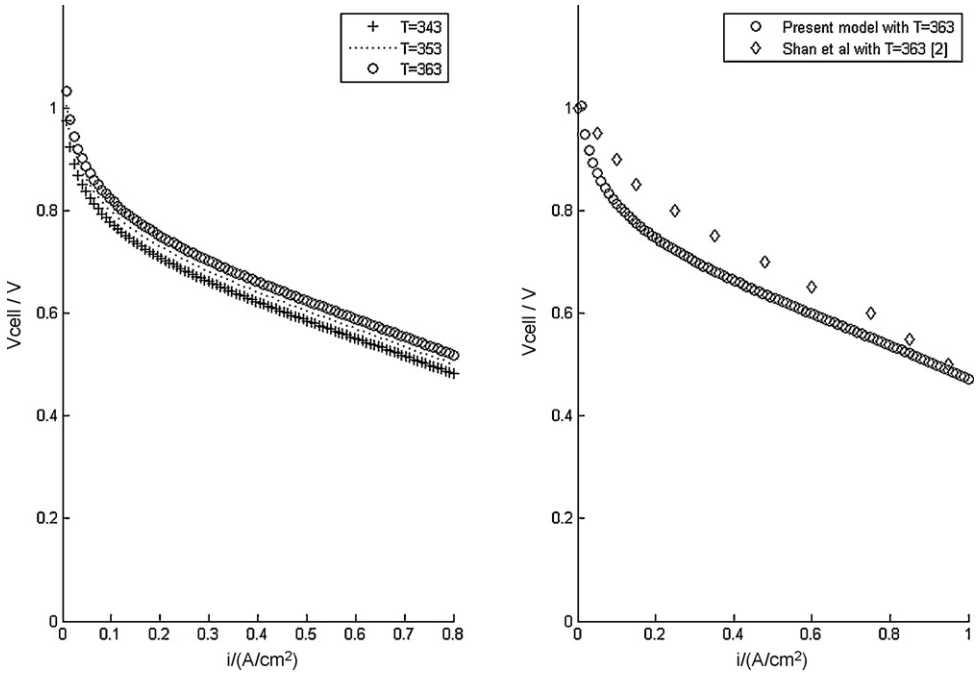


**Fig. 2.** Voltage curve over current density *i*.

$V_{cell}$ are more spread for the Gaussian distribution. This result is expected as for a uniform distribution, each interval of the same length is equally probable.

An analysis of one vertical block of $V_{cell}$ in Fig. 4 at a specific current density of 0.6 A cm$^{-2}$ can be done with its histogram to view the type of distribution of $V_{cell}$ in Fig. 5.

The distribution of $V_{cell}$ seems to be Gaussian for a Gaussian temperature and uniform for a uniform temperature but this visual deduction needs to be proved by a statistical analysis.

For this purpose, the coefficient of variance (COV) which is defined by the division of the standard deviation by the mean will be used. It can be understood as "a certain percentage of uncertainties accepted". For instance we accept 1% of uncertainties on the temperature referring to ref. [29]. The results on the output voltage are at the top of Fig. 6. We can notice that the increase of the coefficient of variance of the output voltage is almost exponential versus current density for both Gaussian and uniform distributions representing a constant COV of 1%. Two additional helpful statistical tools for distributions analysis are the skewness and the kurtosis. Skewness is a measure of the asymmetry of the probability distribution and kurtosis indicates whether a probability distribution is peaked or flat [31]. The mathematical definitions of these two terms are in Appendix A. Skewness of the output voltage in the case of Gaussian and uniform temperature nearly equals to 0 as

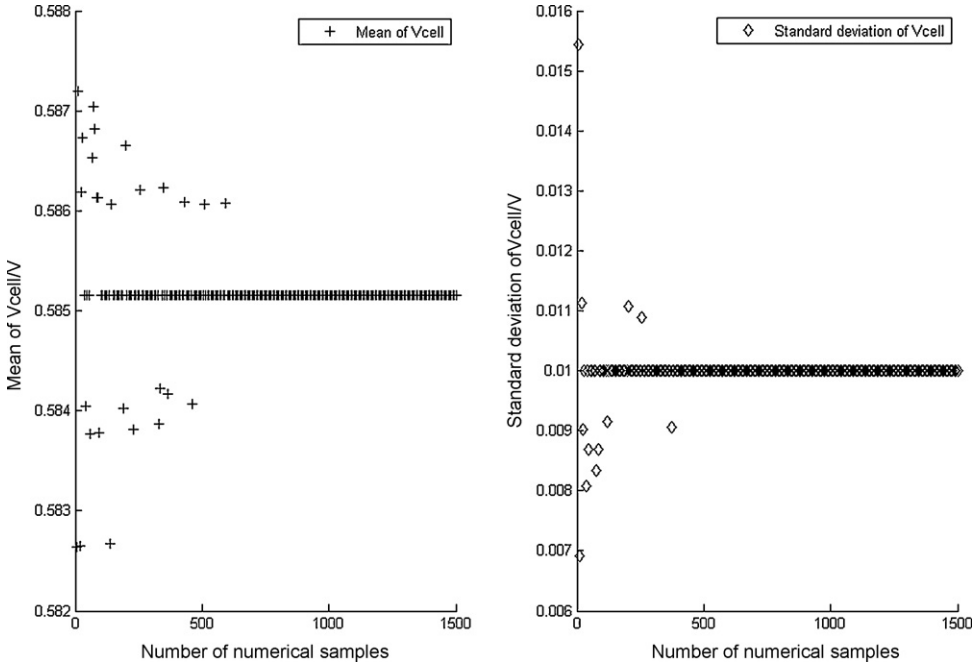


**Fig. 3.** Stochastic convergence analysis of the mean and the standard deviation of $V_{cell}$.

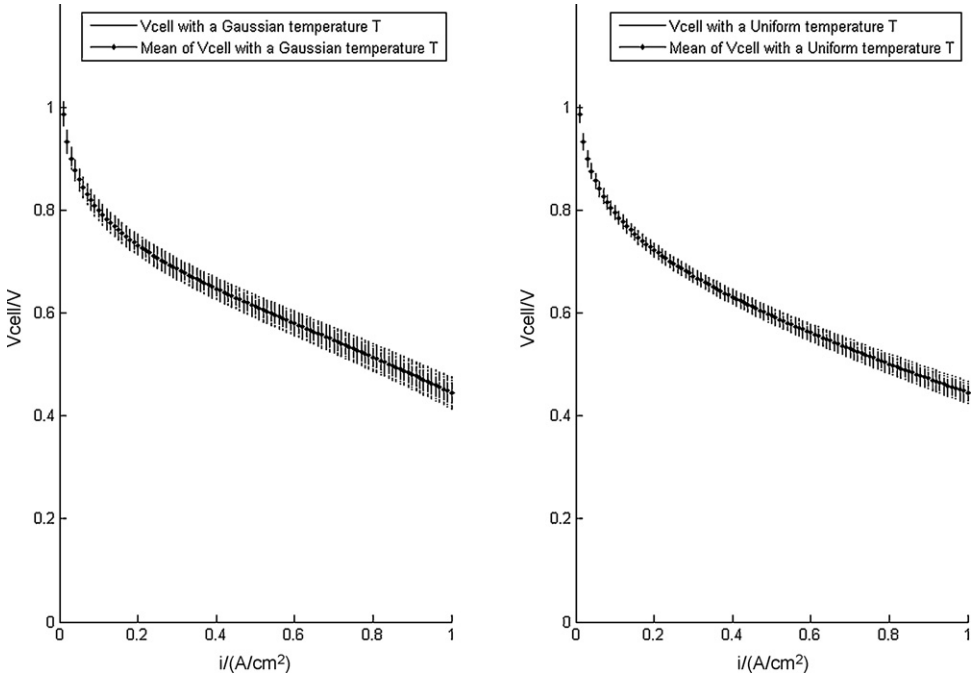


**Fig. 4.** $V_{cell}$ versus current density with a Gaussian (left) and a uniform (right) temperature distribution.

indicated by the second curve of Fig. 6. Finally, the kurtosis of 3 for the Gaussian temperature and 1.8 for the uniform one on the third curve of Fig. 6 confirm that the type of distribution of the output voltage is the one of the input temperature for this model. This result will be confirmed by the results of the work in Section 5, as a linear relationship can be established between $V_{cell}$ and the temperature $T$.

In this model, all the components parameters, notably the cell reactive area A, are assumed to be constant but in real operating conditions, they are subject to degradations and decrease over time [32–34]. A model integrating one characteristic degradation will be studied in the next section.

## 4. Degrading PEM fuel cell model

Many failures modes are encountered during PEM fuel cells operations involving mechanical, thermal and chemical processes. All PEM fuel cell components are subjected to these degradations [32–35] and many efforts have been made to model those degradations. For example, Shah et al. [35] modelled the chemical degradations of the membrane of PEM fuel cells, Meyers and Darling [36] proposed a mathematical model of the corrosion of carbon catalyst supports, Bu et al. [37] studied Pt/C dissolution and deposition in Nafion electrolyte. The degradation processes are complex and difficult to take into account in one model. To simplify the

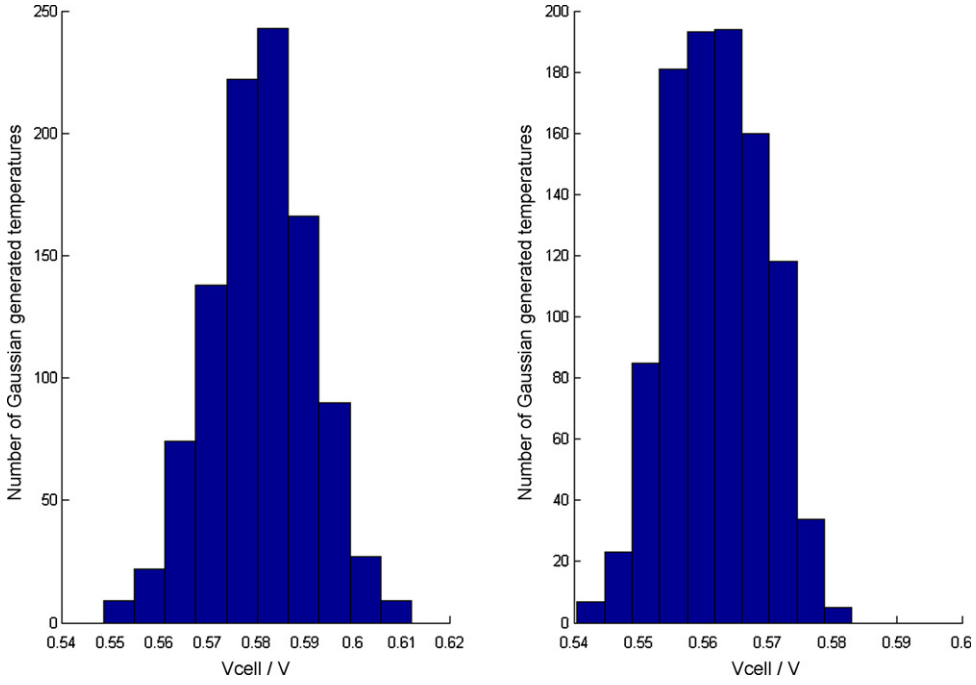


**Fig. 5.** Histogram of $V_{cell}$ for $i = 0.6\,A\,cm^{-2}$ for 1000 Gaussian (left) and uniform (right) distributed temperatures.

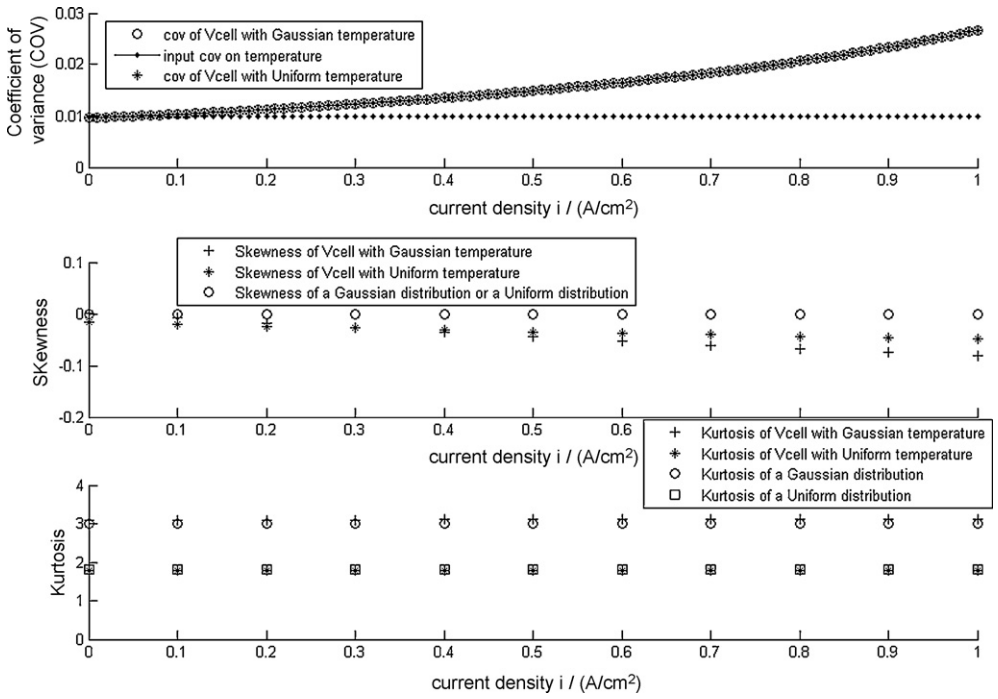


**Fig. 6.** Coefficient of variance, skewness and kurtosis of $V_{cell}$ versus current density with a Gaussian and uniform temperature distribution.

model, only degradations on the cell reactive area are considered and the degradation rate suggested gathers all types of degradation concerning the cell active area. The drop of this surface during cycling has been measured by Tang et al. [38]. These experimental values have been fitted and the resulting model has been taken into account to simulate the decrease of the cell active area A.

### 4.1. Model mathematical equation and its validation

All the expressions are the same as in Section 3 except for the cell reactive area A which follows the expression deduced empirically from Tang et al. [38]:

$$A = 2.5 + 50\ \exp(-k2 \times t) \quad (5)$$

where $k2$ is the degradation rate of the membrane ($h^{-1}$); $t$ is the current time (h).

This modified model will allow to simulate the decrease of the voltage over the current time $t$.

$k2$ is chosen equal to 0.0002 for plotting which is acceptable compared with refs. [19,39]. This expression of the cell active area is coherent with the observations of Tang et al. [38] who noticed that the cell active area was reduced to about 1/3 of its original value after 80 cycles which corresponds approximately to a 2000 h operation in this model. The ageing of the fuel cell will be studied in this section through the representation of the voltage of a cell submitted to a current of 30 A.

Fig. 7 confirms results of refs. [29,30]. A running time $t$ of 3000 h leads to a decrease of the voltage down to 0.43 V which corresponds to the lower tolerated limits for fuel cells.

### 4.2. Integration of uncertainties into the model and analysis

According to Coppo et al. [29], and Mawardi and Pitchumani [30], uncertainties on temperature are a major problem in a PEM fuel cell. So it is interesting to generate randomly a temperature and to analyse the influence on the $V_{cell}$. Next, we can consider the temperature as constant and generate randomly the degradation rate $k2$. Then, both previous cases can be combined to the case when temperature and the degradation rate are randomly generated.

#### 4.2.1. Effects of the temperature uncertainty

The temperature $T$ is assumed to follow a Gaussian distribution with a mean of 353 K and a standard deviation of 3.53 K, then a uniform distribution with 347 and 359 K as lower and upper bounds. The degradation rate of the cell active area $k2$ has a constant value of 0.0002. To ensure the quality of the statistical results, 1000 values of $T$ are generated.

The left-hand side of Fig. 8 shows the spread of $V_{cell}$ for 1000 gaussianly generated temperatures $T$, whereas the right-hand side of Fig. 8 shows the spread of $V_{cell}$ for 1000 uniformly generated temperatures $T$. $V_{cell}$ distribution is more spread in the first case as in the previous model.

It is of interest to analyse one vertical block of the $V_{cell}$ graph, for example at a specific time of 1500 h (half of the overall running time), and to draw its histogram to view the distribution of $V_{cell}$.

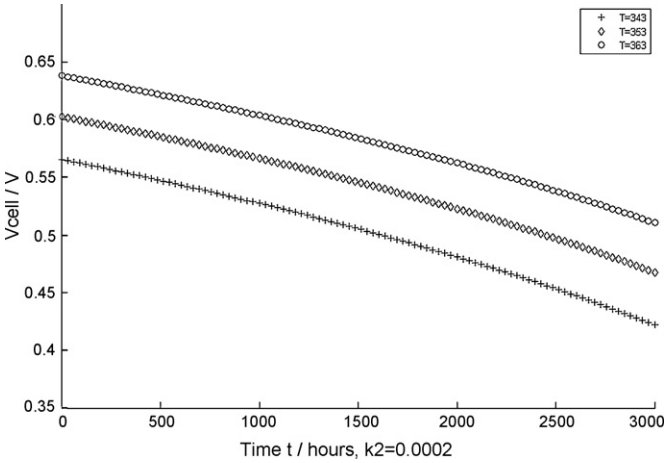


**Fig. 7.** Voltage curve over running time for current $I$ = 30 A at three fixed temperatures.

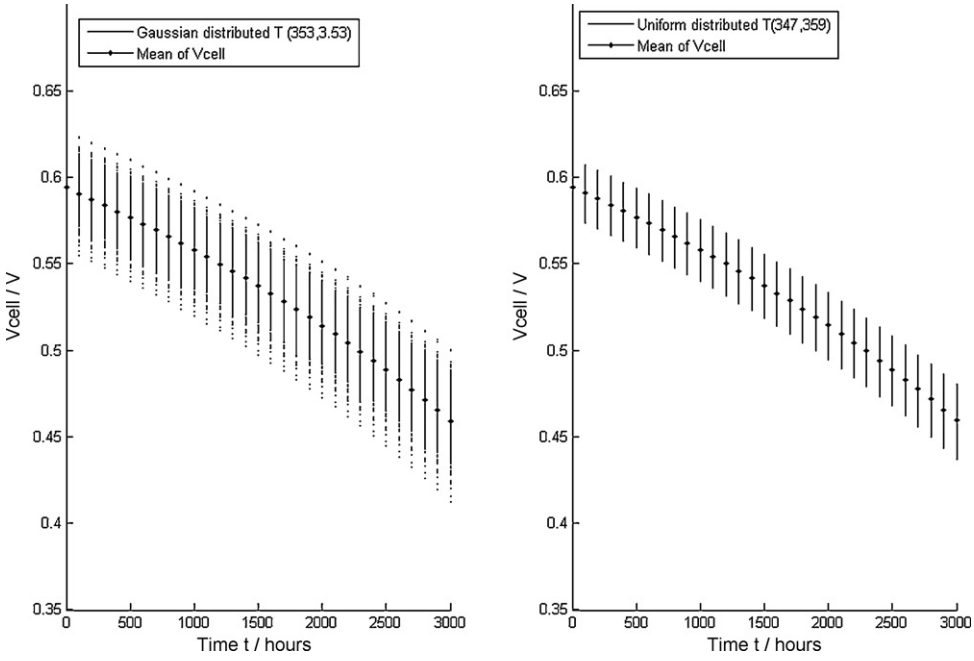


**Fig. 8.** $V_{cell}$ versus time for current $I = 30$ A with randomly distributed temperature.

The histogram on the left-hand side of Fig. 9 shows a Gaussian distribution of $V_{cell}$, with 1000 generated temperatures around the mean (at the centre of the histogram) and few data on the bounds. The right-hand side histogram seems to confirm that $V_{cell}$ is uniformly distributed.

To complete the identification of the distribution type of $V_{cell}$, it is necessary to plot the coefficient of variance (COV), skewness and kurtosis of $V_{cell}$ versus time $t$ with Gaussian and uniform distributed temperatures in Fig. 10.

The first curve of Fig. 10 indicates that an input uncertainty of 1% on the temperature results in an exponential growth of the $V_{cell}$ uncertainty up to 5% while the current time is in the range of 0–3000 h. The second curve of Fig. 10 shows a slight fall of the skewness of $V_{cell}$ for a uniform temperature down to −0.05 and a greater fall for a Gaussian temperature down to −0.1. The different values of the skewness are very close to 0 so the distribution of $V_{cell}$ is nearly symmetric in both cases. The third curve of Fig. 10 clearly shows that the kurtosis of both Gaussian and uniform temperatures cases of $V_{cell}$ remain constant at nearly 3 and 1.8, respectively.

To sum up, the distribution of the output voltage with a Gaussian temperature is nearly Gaussian and in the case of a uniform distribution is nearly uniform because both distributions are not rigorously symmetric. This can have a great influence on the extreme values which will not be Gaussian or uniform. The degradation of the cell active area probably seems to modify slightly the distribution of the output voltage as it is the only difference with

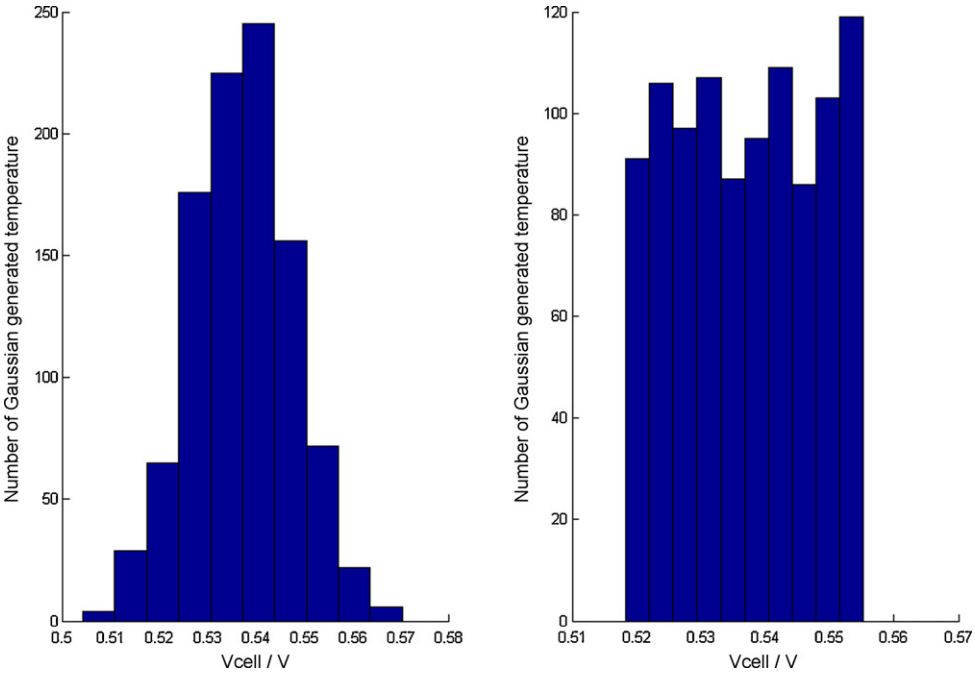


**Fig. 9.** Histogram of $V_{cell}$ at time $t = 1500$ h for randomly distributed temperature.

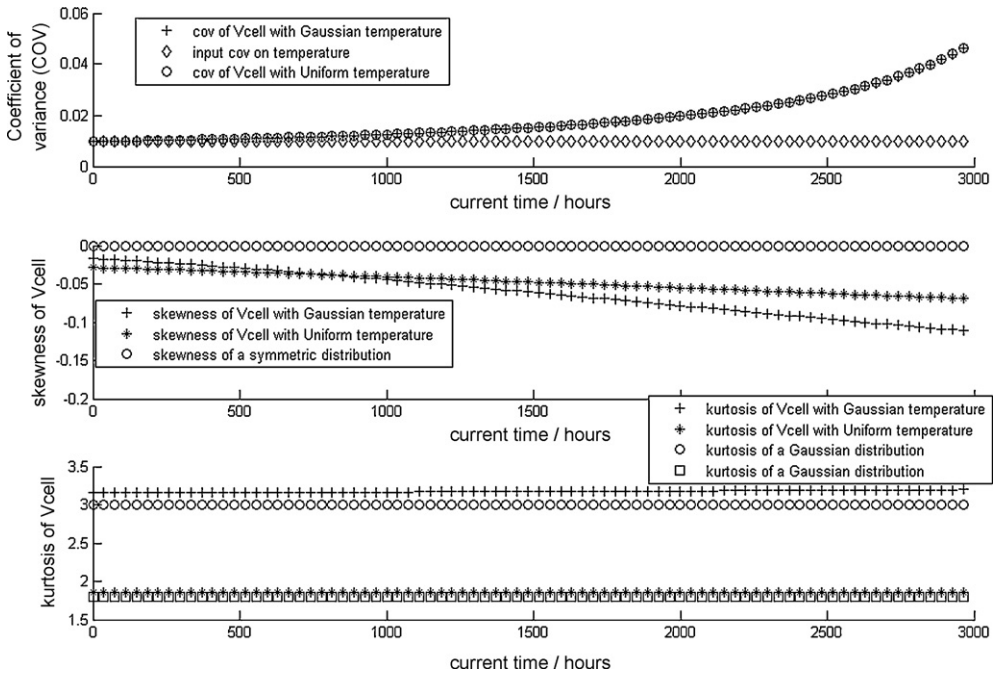


**Fig. 10.** COV, skewness and kurtosis of $V_{cell}$ versus time $t$ with randomly distributed temperature.

the previous model. Degradation rate is an important parameter and needs to be studied.

The next section analyses the effect of a random degradation rate on the output voltage. To achieve this objective, the degradation rate of the cell active area $k2$ is generated randomly while the temperature remains deterministic.

### 4.2.2. Effects of the degradation rate of the cell active area uncertainty

The degradation rate of the cell active area $k2$ is randomly generated as a Gaussian distribution with a mean of 0.0002 and a standard deviation of 0.00002, then as a uniform distribution with 0.000165 and 0.000235 as lower and upper bounds, while the temperature $T$ is assumed to remain constant at 353 K. To ensure the quality of the statistical results, 1000 values of $k2$ are generated.

Fig. 11 emphasises the fact that the dispersion of $V_{cell}$ rises with time. This is an expected result, as the degradation of the cell active area should be more severe in the long-term fuel cell use [19].

It can also be noticed that the degradation on $V_{cell}$ is more spread with the Gaussian temperature than the uniform one. A visual analysis of the output voltage distribution can be done by plotting the histogram in each case at a specific time of 1500 h in Fig. 12.

As found earlier, the distribution of $V_{cell}$ with gaussianly generated degradation rates seems Gaussian and the distribution of $V_{cell}$ with a uniformly generated degradation rates seems uniform.

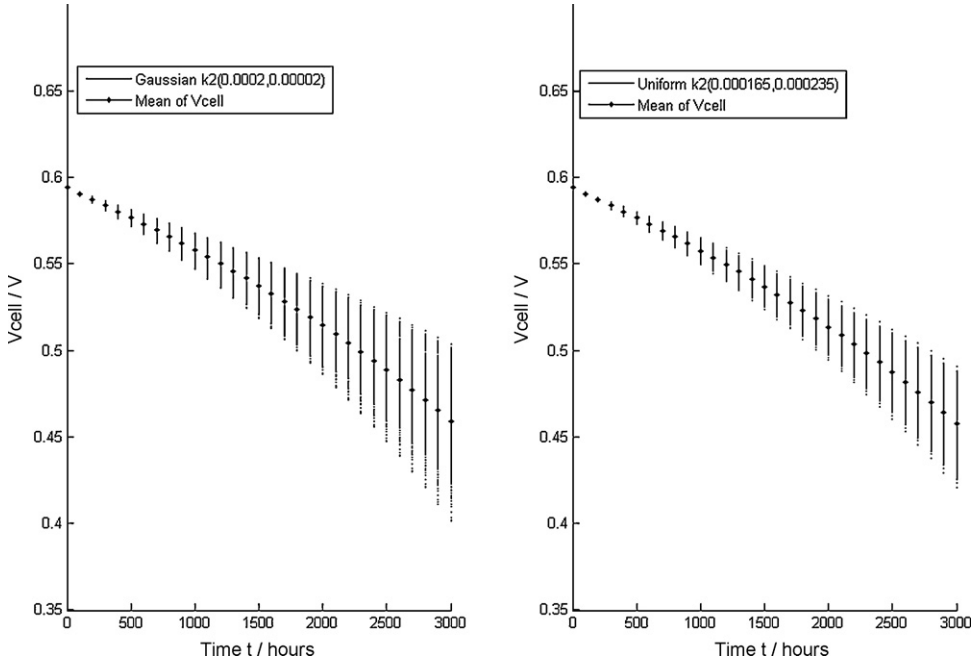


**Fig. 11.** $V_{cell}$ versus time for $I = 30$ A with a randomly distributed degradation rate of the cell active area.

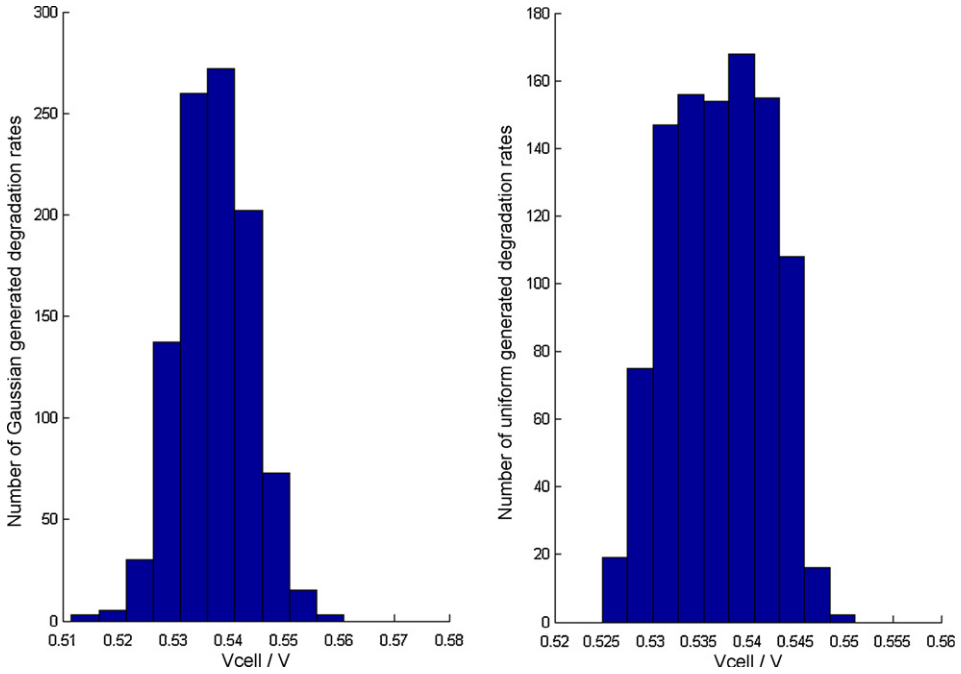


**Fig. 12.** Histogram of $V_{cell}$ at $t$ = 1500 h with randomly distributed $k2$.

The output voltage analysis is displayed on the graphs of the coefficient of variance, the skewness and the kurtosis of $V_{cell}$ over the current time with both stochastical degradation rates $k2$ (Fig. 13).

In the first curve of Fig. 13, 10% of uncertainty on the degradation rate is considered. It is realistic according to ref. [34], the resulting uncertainty on $V_{cell}$ is less than 10% over time. This result can be important for fuel cell designers. Until 2000 h work-in, the skewness of $V_{cell}$ with Gaussian and uniform degradation rates is nearly symmetric meanwhile the kurtosis is 3 and 1.8, respectively.

To conclude, the distribution of the output voltage follows the distribution of the input degradation rate until 2000 h lifetime of the model. This is confirmed by the histogram of Fig. 12 which corresponds to a lifetime of 1500 h. After 2000 h lifetime, with a Gaussian $k2$, the resulting $V_{cell}$ is no more Gaussian and the resulting $V_{cell}$ is no more uniform for a uniform $k2$.

In the next section, the temperature and the degradation rate $k2$ are generated randomly in order to meet real operational conditions in the fuel cell.

### 4.2.3. *Effects of combined uncertainties on the temperature and on the degradation rate of the cell active area*

This case is the combination of both Sections 4.2.1 and 4.2.2 cases, the temperature $T$ and the degradation rate $k2$ of the membrane are assumed to follow a Gaussian and then a uniform distribution with the same parameters as in the previous cases.

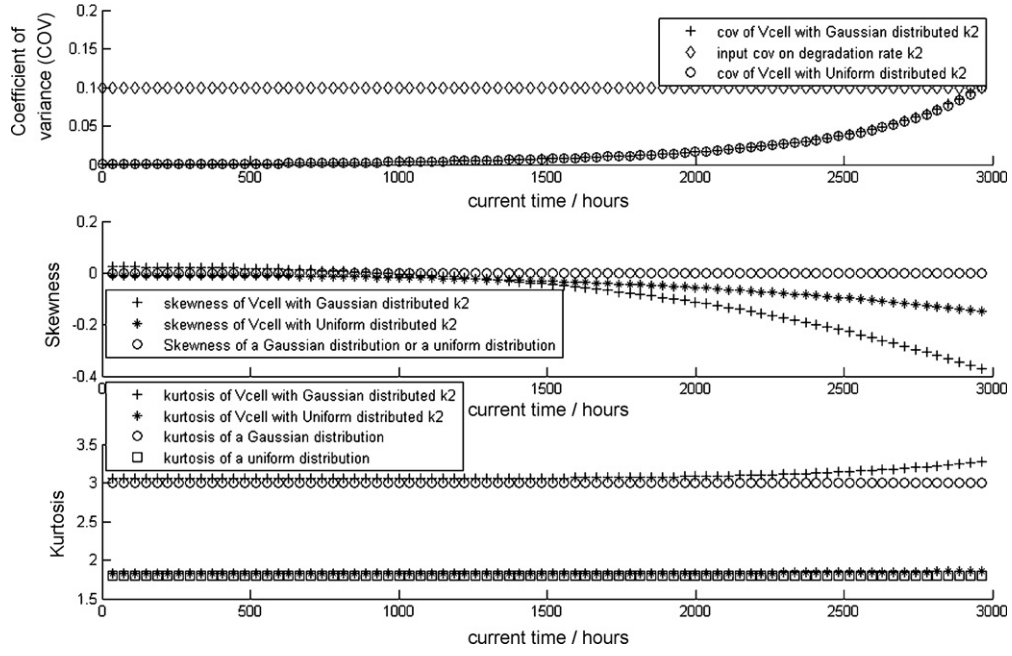


**Fig. 13.** Coefficient of variance, skewness and kurtosis of $V_{cell}$ versus time $t$ with randomly distributed $k2$.

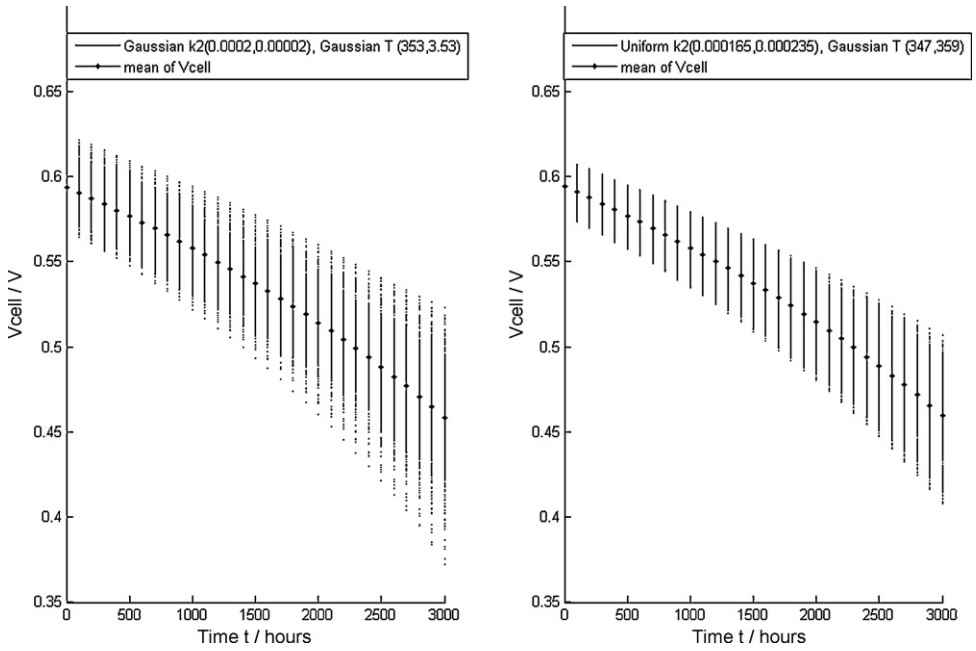


**Fig. 14.** $V_{cell}$ versus time for $I = 30$ A with randomly distributed $T$ and $k2$.

Fig. 14 confirms the observations made about the influence of lifetime on the voltage of the cell as the spread of distributions rises gradually as time runs in both cases.

A visual analysis of Fig. 15 fails because the distribution type is not so obvious as in the previous cases.

To complete this study, it is necessary to plot the coefficient of variance of $V_{cell}$, the skewness, the kurtosis in Fig. 16.

The first curve of Fig. 16 shows that a 1% uncertainty on the input temperature and 10% uncertainty on the input degradation rate result in an exponential growth of the $V_{cell}$ uncertainty higher than 1% but inferior to 10% when the long-term use of the cell is less than 3000 h. A 1% uncertainty on the input temperature and a 10% uncertainty on the input degradation rate are realistic according to refs. [19,30,34].

An analysis of the skewness and kurtosis curves in Fig. 16 shows that up to 1000 h lifetime, the output voltage distribution nearly follows the distribution of the inputs (temperature and degradation rate). After 1000 h lifetime, the resulting output voltage is neither Gaussian for Gaussian inputs, nor uniform for uniform inputs.

It can also be noticed that the different values obtained here are combinations of the first two previous cases.

To analyse the effects of major parameters of this model, the Response Surface Method is used followed by a statistical sensitivity

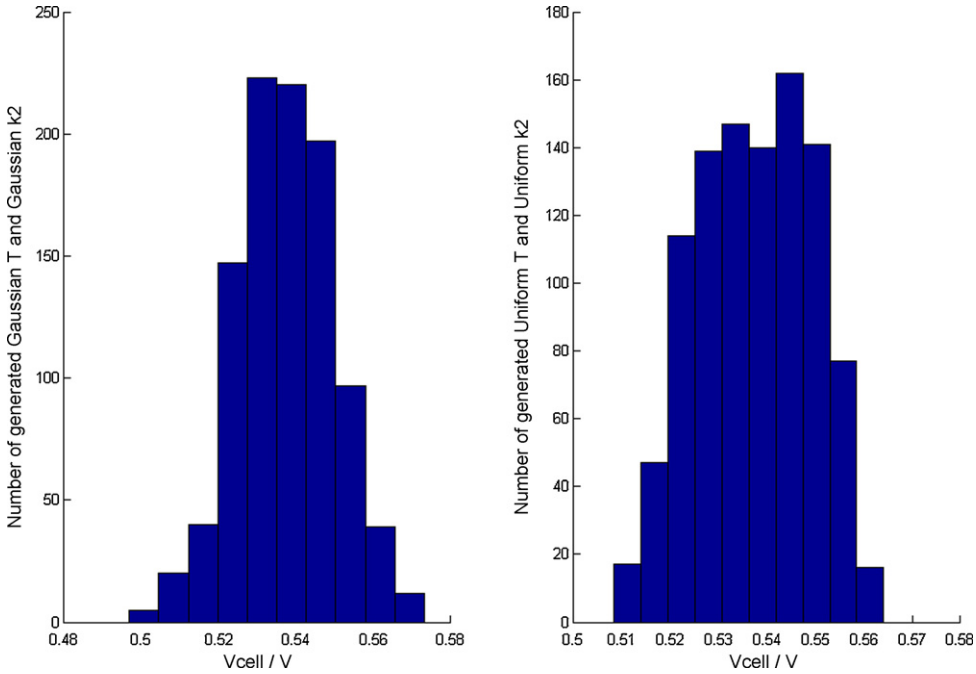


**Fig. 15.** Histogram of $V_{cell}$ at $t = 1500$ h with randomly distributed $T$ and $k2$.

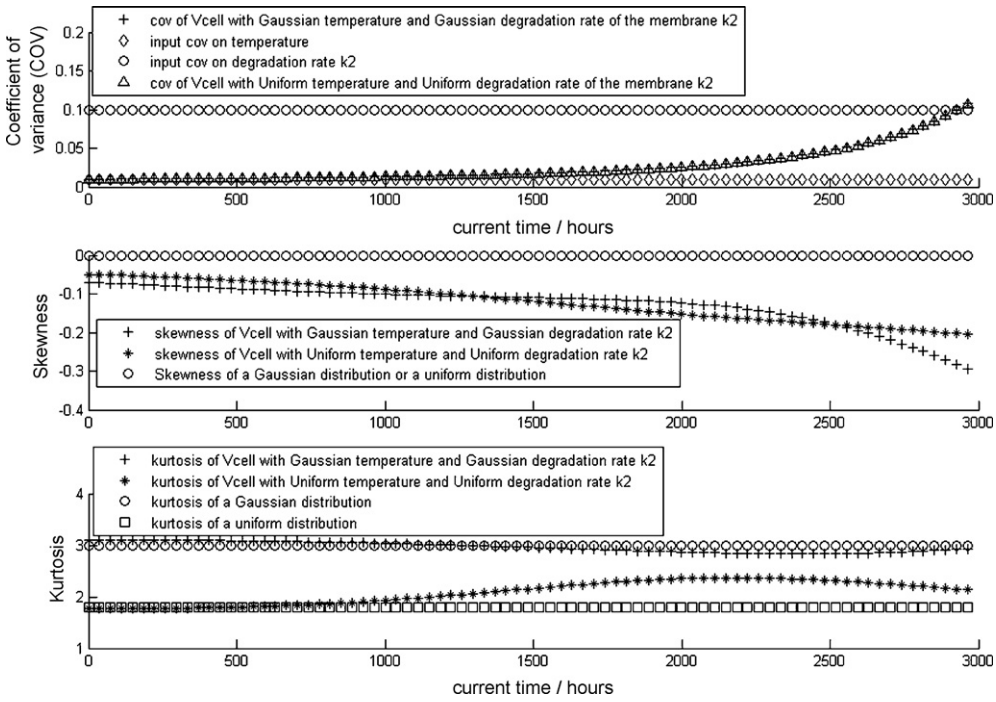


**Fig. 16.** Coefficient of variance, skewness and kurtosis of $V_{cell}$ versus time with randomly distributed temperature and degradation rate of the cell active area.

analysis to compute the contributions of the factors to the fuel cell voltage.

## 5. Full factorial design analysis on the degrading PEM fuel cell model

This section gathers two sub-sections: sub-Sections 5.1 and 5.2. The first one studies the effects of the first order interactions of the major parameters on the fuel cell voltage considering those parameters deterministic. The objective is to conclude whether those interactions are to be taken in account in a design of experiment or not. Once this established, a random design of experiment will be performed on the major parameters for comparison with the results obtained in the first four sections of this work in the second sub-Section 5.2.

### 5.1. Effects of the interaction factors

The Response Surface Method (RSM) estimates the linear effects, the quadratic effects and the interactions of a few important factors chosen before using screening procedures. The general expression of the RSM analytical models is simple when written in a matrix form:

$$\hat{y} = X \cdot \hat{\beta} \tag{6}$$

$y$ is the mathematical function, here $V_{cell}$ of expression (1). It can also be a vector of experimental results. $\hat{y}$ is the vector of the polynomial approximation at each experimental point (in fact, $y = \hat{y} + \varepsilon$). $\varepsilon$ corresponds to the fitting error. $X$ is the design matrix and depends on the numerical point position and on the type of polynomial model used. $\hat{\beta}$ is the estimated coefficient vector.

$$\hat{\beta} = (X^t \cdot X)^{-1} \cdot X^t \cdot y \tag{7}$$

For this work, a quadratic regression is used to fit the data and the coefficients are obtained by minimizing the square of the error.

$$\hat{V}_{cell} = \beta_0 + \beta_1 T + \beta_2 k2 + \beta_3 t + \beta_4 T^2 + \beta_5 (k2)^2 + \beta_6 t^2 + \beta_7 T \cdot k2 + \beta_8 T \cdot t + \beta_9 k2 \cdot t \tag{8}$$

where $\beta_i$, $i = 0, \ldots, 9$ are the factor effects.

**Table 4**
Factor effects on the fuel cell voltage.

| Factor effects | Values |
|---|---|
| $\beta_0$ | 5.5323355e−001 |
| $\beta_1$ | −1.1791774e−002 |
| $\beta_2$ | −4.2488864e−003 |
| $\beta_3$ | 7.5509077e−003 |
| $\beta_4$ | −3.6824034e−004 |
| $\beta_5$ | −6.5639348e−005 |
| $\beta_6$ | −5.6995501e−005 |
| $\beta_7$ | −1.2063074e−003 |
| $\beta_8$ | 1.6778221e−004 |
| $\beta_9$ | 6.3046959e−005 |

Here the lifetime factor $t$ will have nine levels, and factors $T$ and $k2$ will have three levels as stated in the chart below.

The number of numerical experiments is $9 \times 3 \times 3 = 81$ for all combinations of $t$, $T$ and $k2$ levels.

The results of the factor effects $\beta_i$, $i = 0, \ldots, 9$ found are in Table 4.

The ANOVA analysis [40] (Fig. 17) proves that the influence of all the first order interactions is less than 6% which is negligible, so we can simplify Eq. (8) into the following equation:

$$\hat{V}_{cell} = \beta_0 + \beta_1 T + \beta_2 k2 + \beta_3 t \tag{9}$$

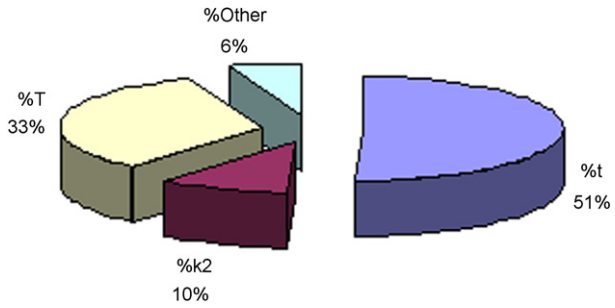


**Fig. 17.** Contributions of each factor to the fuel cell voltage.

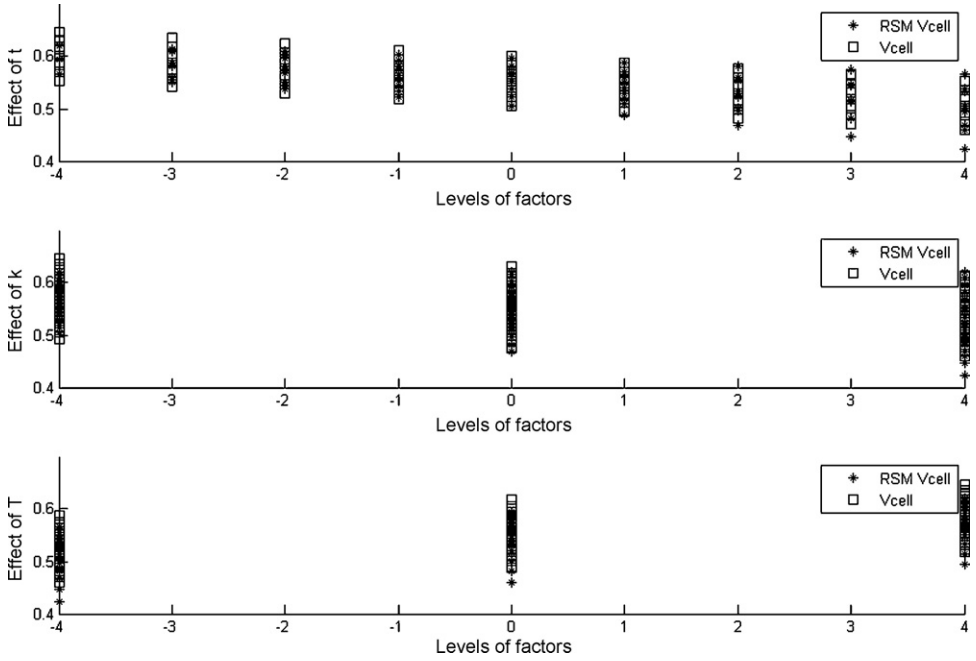


**Fig. 18.** Effects of each factor $t$, $k2$ and $T$ using Eq. (9).

Fig. 18 represents the effects of each factor $t$, $k2$ and $T$ using the new Eq. (9): the first curve shows that $V_{cell}$ decreases with lifetime $t$, the second curve indicates that $V_{cell}$ falls with a rising degradation rate $k2$ and the last curve shows that $V_{cell}$ increases with the temperature $T$. The results of Fig. 18 agree with the results of the simulation part.

$R^2$ is the multiple regression correlation and is very important in statistical modelling. This coefficient is between 0 and 1. A value close to zero involves a poor model whereas a value of 1 means that the model exactly fits the measurement and totally explains the studied phenomenon.

For this model with Eq. (9), we found $R^2 = 0.987$ which shows the accuracy of this model.

The most important factors are $t$, $k2$ and $T$. To complete the design of experiment, each factor will be considered with its mean and its standard deviation. So there will be six factors for a two-level full factorial design which requires 64 runs ($2^6$). Each factor will be randomly generated 1000 times and then an ANOVA analysis will be done on the output voltage. All the factor levels are chosen based on the results of the first part of this work in order to avoid an overlap in the output voltage and to cover the region of interest.

### 5.2. Random full design analysis and results

A full design analysis for the degrading PEM fuel cell model is used by considering six main factors and each of them at two levels, the details of which are given in Table 5.

**Table 5**
Levels of the main factors.

| Factors | Parameters | Lower level | Upper level |
|---|---|---|---|
| $mt$ | Mean of $t$ (h) | 750 | 2250 |
| $st$ | Standard deviation of $t$ | 0.1 | 0.2 |
| $mk2$ | Mean of $k2$ | $10^{-4}$ | $2 \times 10^{-4}$ |
| $sk2$ | Standard deviation of $k2$ | 0.1 | 0.2 |
| $mT$ | Mean of $T$ | 343 | 363 |
| $sT$ | Standard deviation of $T$ | 0.01 | 0.08 |

The other parameters remain the same as in the simulation section of this work. Each treatment combination is replicated 1000 times.

Fig. 19 represents the effects of each of the six factors on the output voltage.

Concerning the first factor, the graph on the first line in the first column from the left clearly indicates that a higher lifetime results in a lower and more spread mean of $V_{cell}$. Below this graph in the same column, as expected the standard deviation of $V_{cell}$ increases with the mean of lifetime on the second graph. The third graph of the same column shows a skewness around 0 for a lifetime less than 1000 h and very spread after 2000 h. Before 1000 h lifetime, the skewness is nearly a symmetric distribution's skewness and after a long run work-in (2000 h), the skewness is no longer a symmetric distribution skewness. As for the skewness graph, the kurtosis one shows a nearly Gaussian distribution before 1000 h and a not Gaussian distribution after 2000 h. In addition, the kurtosis rises slightly with mean of time. These results on the skewness and the kurtosis are acceptable compared with results of the simulation part in Section 4.2.3.

The effects of the mean of the degradation rate $k2$ on the $V_{cell}$ distribution are represented in the second column of Fig. 19. The mean of $V_{cell}$ decreases with a higher degradation rate on the first graph of this column and is more spread with a rising mean of $k2$ which is confirmed by the second graph. The third graph of the same column shows that the skewness of $V_{cell}$ declines slightly with a high mean of $k2$ and the fourth one indicates that the kurtosis remains almost constant. The skewness and the kurtosis results confirm results found in Section 4.2.2 of the simulation part.

The third column of Fig. 19 analyses the effects of the mean of temperature $T$. The first graph of this column shows a climb of the mean of $V_{cell}$ with a higher temperature and the second one points out a slight decline of the standard deviation. This is coherent with the results of Section 4.2.1 while analysing the graph of the coefficient of variance (COV). The third and the fourth graphs of this column indicate a nearly Gaussian distribution for a rising temperature $T$ which confirms the results of Section 4.2.1.

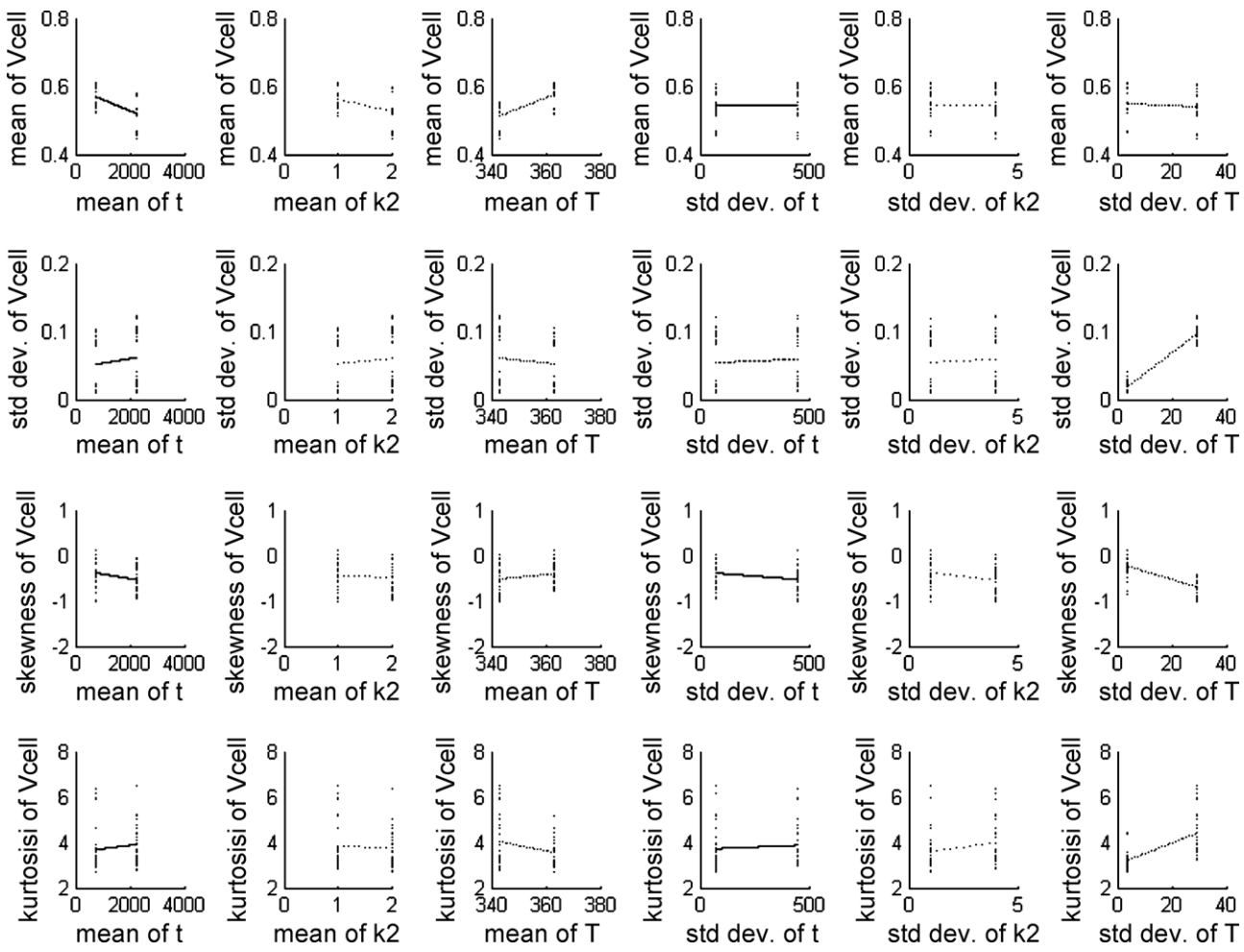


**Fig. 19.** Effects of each of the six factors on the output voltage.

The effects of the standard deviation of the current time $t$ are described by the graphs in the fourth column of Fig. 19. According to the first and the second graphs of this column, the mean and the standard deviation of $V_{cell}$ remain relatively constant with an increasing standard deviation of lifetime $t$. The third graph and the fourth graph indicate respectively a slight drop of the skewness of $V_{cell}$ and the kurtosis of $V_{cell}$ does not change with a rising standard deviation.

The fifth column of Fig. 19 describes the effects of the standard deviation of the degradation rate $k2$. Referring to the first and the second graphs of this column, the mean and the standard deviation of $V_{cell}$ remain relatively constant with an increasing standard deviation of $k2$. The third graph indicates a slight drop of the skewness of $V_{cell}$ and the kurtosis of $V_{cell}$ slightly increases with a rising standard deviation on the fourth graph.

Finally, the last column of Fig. 19 represents the influence of the standard deviation of the temperature $T$ on $V_{cell}$ distribution. The mean of $V_{cell}$ slightly decreases with an increased standard deviation of the temperature on the first graph. The standard deviation of $V_{cell}$ rises with the standard deviation of the temperature on the second graph. The skewness of $V_{cell}$ goes down with an increasing standard deviation on the temperature on the third graph meanwhile the kurtosis of $V_{cell}$ climbs on the last graph. With a low standard deviation on the temperature (variability of 1%), the resulting voltage distribution seems to be symmetric but with a higher variability (8%), it is no longer symmetric. The results on the kurtosis are similar: with a variability of 1%, the voltage distribution seems to be Gaussian and at a variability of 8% is no more Gaussian. The contributions of each of these six factors to the mean, standard deviation, skewness and kurtosis of $V_{cell}$ are listed in Table 6.

**Table 6**
Contribution of each of the main factors to the mean, standard deviation, skewness and kurtosis of $V_{cell}$.

| Factors | Contributions to the | | | |
|---|---|---|---|---|
| | Mean of $V_{cell}$ (%) | Standard deviation of $V_{cell}$ (%) | Skewness of $V_{cell}$ (%) | Kurtosis of $V_{cell}$ (%) |
| *mt* | 30.322112 | 1.434557 | 2.440295 | 0.406626 |
| *st* | 0.013962 | 0.273815 | 3.971078 | 0.529764 |
| *mk2* | 14.540507 | 0.789673 | 4.673607 | 3.253045 |
| *sk2* | 0.025757 | 0.381841 | 5.113494 | 1.976349 |
| *mT* | 48.507651 | 1.049 | 3.852172 | 4.860403 |
| *sT* | 1.189434 | 94.211099 | 48.092272 | 34.890808 |
| Error | 5.400578 | 1.872751 | 31.857082 | 54.083006 |

This full factorial analysis helps to specify which of the six parameters have a considerable effect on the output voltage. According to Table 6, the means of lifetime, temperature and degradation rate contribute with more than 93% to the mean of $V_{cell}$ and the standard deviation of temperature explains more than 94% of the standard deviation of $V_{cell}$. In addition, it is difficult to conclude on the skewness and kurtosis of $V_{cell}$ by only considering the six previous factors because the error involved is respectively more than 30% and more than 50%. The four important parameters from this analysis for PEM fuel cell design are: the mean of lifetime $t$, the mean of the degradation rate $k2$, the mean and the standard deviation of the temperature $T$.

## 6. Conclusion

This work contributes to the knowledge concerning the influence of temperature uncertainties on the voltage output of a proton exchange membrane fuel cell. The first model does not include any degradation and helps to consider the involvements due only to the temperature. With a randomly distributed temperature, it comes out that the cell output voltage of the model seems to follow the distribution of the input temperature. The second model takes into account a degradation rate of the active cell area with time. In this case, with a Gaussian and a uniform distribution of the temperature, the resulting voltage distribution is respectively nearly Gaussian and uniform. The fact that the resulting voltage distribution does not rigorously follow the input distribution of the temperature proves that the degradation rate is an important parameter to consider. So the case with a randomly generated degradation rate of the membrane and a constant temperature was studied. It comes out that until 2000 h of lifetime; the output voltage follows the distribution of the input distribution of the degradation rate. After 2000 h, it is no longer true. With this second case, it becomes necessary to study the combinations of both cases: the temperature and the degradation rate following both a Gaussian distribution and then a uniform distribution. The fuel cell model shows that until 1000 h of current time the resulting voltage follows the distribution of the inputs and after 1000 h, it is no longer the case. Current time is also important in this model. To complete the previous simulation work, a RSM method is used to study the effects of interactions of the three most important parameters which are the temperature $T$, the degradation rate $k2$ and the current time $t$. The objective of the method is to determine if the output voltage can be represented with a polynomial expression of those parameters that fits the results of the simulation. The interactions between the three parameters are proved to be negligible and a linear expression of the three parameters fits well the simulated output voltage. To improve the knowledge on the specific part of the parameter that has an important effect on the output voltage, each parameter is split into two parts: its mean and its standard deviation.

To allow comparisons with the simulations, a random full design of experiment is performed on the six new parameters. The results confirm the simulations. Furthermore, three parameters are proved to have the most important effects on the mean of the output voltage: the mean of lifetime $t$, the mean of the degradation rate $k2$, the mean of the temperature $T$. As far as the standard deviation of $V_{cell}$ is concerned, the standard deviation of the temperature has the greatest contribution.

The results of this work are interesting for designing PEM fuel cell and the methodology introduced here can be applied to more realistic models by considering more parameters subject to uncertainty. However, researchers should be aware of the fact that implementing this method on complex models with many uncertain parameters will need greater computational requirements.

## Appendix A. Statistical tools [31]

### A.1. Gaussian or normal distribution

The *normal distribution*, also called the *Gaussian distribution*, is a two-parameter family of curves: the first parameter which is the location parameter is the mean ("average", $\mu$) and the second parameter which is the scale parameter is the standard deviation ($\sigma$). The *standard normal distribution* is the normal distribution with a mean of zero and a standard deviation of one.

### A.2. Continuous uniform distribution

The continuous uniform distribution is a family of probability distributions such that for each member of the family, all intervals of the same length on the distribution's support are equally probable. The support is defined by the two parameters, $a$ and $b$, which are its minimum and maximum values. The distribution is often abbreviated $U(a, b)$.

The probability density function is a horizontal line segment between $a$ and $b$ at $1/(b-a)$.

$$f(x) = \begin{cases} \dfrac{1}{b-a}, & a \le x \le b \\ 0, & x < a, x > b \end{cases} \tag{a1}$$

### A.3. Skewness

Skewness is defined as a measure of the lack of symmetry of a probability distribution of a real-valued random variable.

Skewness, the third standardized moment, is written as $\gamma_1$ and defined as

$$\gamma_1 = \frac{\mu_3}{\sigma^3} \tag{a2}$$

where $\mu_3$ is the third moment about the mean and $\sigma$ is the standard deviation.

Larger values in magnitude indicate more skewness in the distribution of observations.

### A.4. Kurtosis

Kurtosis describes the extent of the peak in a distribution. Smaller values (in magnitude) indicate a flatter, more uniform distribution. Higher kurtosis means more of the variance is due to infrequent extreme deviations, as opposed to frequent modestly sized deviations.

Kurtosis, the fourth standardized moment is defined as:

$$\text{kurtosis} = \frac{\mu_4}{\sigma^4} \tag{a3}$$

where $\mu_4$ is the fourth moment about the mean and $\sigma$ is the standard deviation.

A high kurtosis distribution has a sharper "peak" and fatter "tails", while a low kurtosis distribution has a more rounded peak with wider "shoulders".

### A.5. ANOVA analysis

Analysis of variance is a statistical procedure for summarizing a classical linear model; a decomposition of sum of squares into a component for each source of variation in the model along with the $F$-test of the hypothesis that any given source of variation in the model is zero. ANOVA can be extended in two different ways when applied to generalized linear models, multilevel models and other extensions of classical regression: the first one is to use the $F$-test to compare nested models, to test the hypothesis that the simpler

of the models is sufficient to explain the data, the second way is to interpret the variance decomposition as an inference for the variances of batches of parameters (sources of variation) in multilevel regressions. Ref. [40] details the different types of ANOVA analysis.

## References


[1] J. Larminie, A. Dicks, Fuel Cell Systems Explained, Wiley, West Sussex, England, 2000.
[2] Y. Shan, S.-Y. Choe, J. Power Sources 145 (2005) 30–39.
[3] E. Barendrecht, in: L.J.M.J. Blomen, M.N. Mugerwa (Eds.), Fuel Cell Systems, Plenum Press, New York, 1993.
[4] J.H. Lee, T.R. Lalk, A.J. Appleby, J. Power Sources 70 (1998) 258–268.
[5] T.V. Nguyen, R.E. White, J. Electrochem. Soc. 140 (8) (1993) 2178–2186.
[6] T.A. Zawodzinski, C. Derouin, S. Radzinski, R.J. Sherman, V.T. Smith, T.A. Springer, S. Gottesfeld, J. Electrochem. Soc. 140 (April (4)) (1993) 1041–1047.
[7] D.M. Bernadi, M.W. Verbrugge, AIChE J. 37 (8) (1991) 1151–1163.
[8] D.M. Bernadi, M.W. Verbrugge, J. Electrochem. Soc. 139 (9) (1992) 2477–2745.
[9] T.E. Springer, T.A. Zawodzinski, S. Gottesfeld, J. Electrochem. Soc. 138 (8) (1991) 2334–2342.
[10] T.E. Springer, M.S. Wilson, S. Gottesfeld, J. Electrochem. Soc. 140 (12) (1993) 3513–3526.
[11] J.J. Baschuk, X. Li, J. Power Sources 86 (2000) 181–196.
[12] A. Rowe, X. Li, J. Power Sources 102 (2001) 82–96.
[13] V. Mishra, F. Yang, R. Pitchumani, J. Power Sources 141 (2005) 47–64.
[14] A. Mawardi, F. Yang, R. Pitchumani, ASME J. Fuel Cell Sci. Technol. 2 (2005) 121–135.
[15] C.H. Min, Y.L. He, X.L. Liu, B.H. Yin, W. Jiang, W.Q. Tao, J. Power Sources 160 (2006) 374–385.
[16] K. Subramanyan, U.M. Diwekar, A. Goyal, J. Power Sources 132 (2004) 99–112.
[17] Wei-Lung Yu, Sheng-Ju Wu, Sheau-Wen Shiah, Int. J. Hydrogen Energy 33 (2008) 2311–2332.
[18] Sheng-Ju Wu, Sheau-Wen Shiah, Wei-Lung Yu, Renewable Energy 34 (2009) 135–144.
[19] M.W. Fowler, Ronald F. Mann, John C. Amphlett, Brant A. Peppley, Pierre R. Roberge, J. Power Sources 106 (2002) 274–283.
[20] P. Bernstein, Against the Gods: The Remarkable Story of Risk, John Wiley & Sons, Inc., New York, NY, 1998.
[21] L. Hacking, The Emergence of Probability: A Philosophical Study of Early Ideas About Probability, Induction and Statistical Inference, Cambridge University Press, Cambridge, United Kingdom, 1984.
[22] J. Murray, The Oxford English Dictionary, vol. XI, Clarendon Press, Oxford, United Kingdom, 1961, pp. U78–U79.
[23] D. Thunnissen, Proceedings of the 3rd Annual Predictive Methods Conference, Veros Software, Santa Ana, CA, June, 2003.
[24] G. Klir, T. Folger, "Types of Uncertainty", Fuzzy Sets, Uncertainty, and Information, Prentice Hall, Englewood Cliffs, NJ, 1988, pp. 138–139.
[25] INCOSE Systems Engineering Handbook, Version 2.0, International Council on Systems Engineering (INCOSE), July 2000.
[26] F. Laurencelle, R. Chahine, J. Hamelin, et al., Fuel Cells (1) (2001) 66–71.
[27] W. Vielstich, A. Lamm, H.A. Gasteiger, Handbook of Fuel Cells: Fundamentals, Technology and Applications. Vol. 3. Fuel Cell Technology and Applications, Wiley Corp., Chichester, England, 2003, ISBN 0-471-49926-9.
[28] M.G. Santarelli, M.F. Torchio, P. Cochis, J. Power Sources 159 (2006) 824–835.
[29] M. Coppo, N.P. Siegel, M.R. von Spakovsky, J. Power Sources 159 (2006) 560–569.
[30] A. Mawardi, R. Pitchumani, J. Power Sources 160 (2006) 232–245.
[31] S. Kokoska, D. Zwillinger, Standard Probability and Statistics Tables and Formulae, Chapman & Hall/CRC, USA, 2000, ISBN 0-8493-0026-6.
[32] A. Collier, H. Wang, X. Yuan, J. Zhang, D.P. Wilkinson, Int. J. Hydrogen Energy 31 (2006) 1838–1854.
[33] A.B. LaConti, M. Hamdan, R.C. McDonald, in: W. Vielstich, H.A. Gasteiger, A. Lamm (Eds.), Handbook of Fuel Cells: Fundamental Technology and Applications, vol. 3, John Wiley & Sons Ltd., 2003, pp. 647–662.
[34] J. Wu, X.Z. Yuan, J.J. Martin, H. Wang, J. Zhang, J. Shen, S. Wu, W. Merida, J. Power Sources 184 (2008) 104–119.
[35] A.A. Shah, T. Ralph, F.C. Walsh, J. Electrochem. Soc. 156 (2009) B465–B484.
[36] J. Meyers, R. Darling, J. Electrochem. Soc. 153 (2006) A1432–A1442.
[37] W. Bi, G.E. Gray, T.F. Fuller, Electrochem. Solid-State Lett. 10 (2007) B101–B104.
[38] Hao Tang, Zhigang Qi, Manikandan Ramani, John F. Elter, J. Power Sources 158 (2006) 1306–1312.
[39] B. Du, R. Pollard, J. Elter, Proceedings of Fuel Cell Seminar 2006, Honolulu/Hawaii/USA, November, 2006, pp. 61–64.
[40] A. Gelman, J. Hill, Applied Regression and Multilevel (Hierarchical) Models, Cambridge University Press, 2006.